ORIGINAL ARTICLE
Basic Medical Sciences

JKMS

http://dx.doi.org/10.3346/jkms.2012.27.8.849 • J Korean Med Sci 2012; 27: 849-856

Portable Document Format File Showing the Surface Models of Cadaver Whole Body

Dong Sun Shin[1], Min Suk Chung[1], Jin Seo Park[2], Hyung Seon Park[3], Sangho Lee[3], Young Lae Moon[4], and Hae Gwon Jang[5]

[1]Department of Anatomy, Ajou University School of Medicine, Suwon; [2]Department of Anatomy, Dongguk University College of Medicine, Gyeongju; [3]Korea Institute of Science and Technology Information, Daejeon; [4]Department of Orthopedics, Chosun University Hospital, Gwangju; [5]Graduate School of Information and Communication, Ajou University, Suwon, Korea

Received: 3 March 2012
Accepted: 25 May 2012

Address for Correspondence:
Hae Gwon Jang
Graduate School of Information and Communication, Ajou University, 164 Worldcup-ro, Suwon 443-749, Korea
Tel: +82.31-219-5027, Fax: +82.31-219-5039
E-mail: crjang@ajou.ac.kr

This study was supported by a grant of the Korean Health Technology R&D Project, Ministry of Health & Welfare, Republic of Korea. (No. A110348).

In the Visible Korean project, 642 three-dimensional (3D) surface models have been built from the sectioned images of a male cadaver. It was recently discovered that popular PDF file enables users to approach the numerous surface models conveniently on Adobe Reader. Purpose of this study was to present a PDF file including systematized surface models of human body as the beneficial contents. To achieve the purpose, fitting software packages were employed in accordance with the procedures. Two-dimensional (2D) surface models including the original sectioned images were embedded into the 3D surface models. The surface models were categorized into systems and then groups. The adjusted surface models were inserted to a PDF file, where relevant multimedia data were added. The finalized PDF file containing comprehensive data of a whole body could be explored in varying manners. The PDF file, downloadable freely from the homepage (http://anatomy.co.kr), is expected to be used as a satisfactory self-learning tool of anatomy. Raw data of the surface models can be extracted from the PDF file and employed for various simulations for clinical practice. The technique to organize the surface models will be applied to manufacture of other PDF files containing various multimedia contents.

Key Words: Models, Anatomic; Image Processing, Computer-Assisted; Imaging, Three-Dimensional; User-Computer Interface; Visible Human Projects

INTRODUCTION

The Visible Korean project was conceived, and has succeeded, in producing three-dimensional (3D) surface models of diverse human structures, with the goal of providing a valuable resource for electronic-based learning of anatomy. In the Visible Korean project, the whole body of a male cadaver (age, 33 yr; cause of death, pneumonia; height, 1.64 m; weight, 55 kg) was serially sectioned and photographed (1). Borders of detailed components were drawn on the sectioned images at 1 mm intervals (2, 3). The outlines of each component were accumulated in sequence and surface reconstruction was executed to build the surface model (2, 4-10).

One of the considerations with this project was how 642 surface models of the subject could be efficiently distributed and visualized (Table 1). Our first decision was that the 3D models needed to be available for viewing off-line. Hollow surface models have a smaller file size than the volume models. However, on-line manipulation of hundreds of surface models cannot be done in real-time. An additional issue is that the Internet handling of the surface models requires the installation of a specific plug-in, which is unnecessary for off-line work.

These considerations led us to ponder the use of the portable document format (PDF) file, which would enable convenient user interaction with the surface models. By nature, the surface models can be seen on the specific 3D viewers like Maya, version 2012 (Autodesk, Inc., San Rafael, CA, USA) (2, 4-10). However, such software is expensive and hard to install on an individual computer. Instead, surface models presented as one-page single PDF file, are effortlessly readable using Adobe Reader, version 9 (Adobe Systems, Inc., San Jose, CA, USA). Adobe Reader provides useful functions to select and rotate the surface models, to obtain 3D views. In addition, two-dimensional (2D) surface models showing the original sectioned images can be embedded in the 3D surface models. Moreover, other multimedia data such as texts, pictures, movies, and voices that are related to the surface models can be attached to the PDF file to provide a rich informational experience for users. Using Acrobat 9.0 Pro Extended (Adobe Systems), these individual surface models in the PDF file can be extracted and utilized for other purposes.

The principal aim of this study was the creation and release of an information-rich and educationally-valuable PDF file in-

pISSN 1011-8934
eISSN 1598-6357

Table 1. Six-hundreds forty-two surface models, categorized according to the systems and subsequent groups

Systems	Groups	Structures
Integumentary (7)		Skin of whole body†, Skin of head & neck†, Skin of trunk†, Skin of upper limb*,†, Skin of lower limb*,†
Muscular (286)	Muscles of head & neck (50)	Buccinator*, Masseter*, Temporal muscle*, Lateral pterygoid muscle*, Medial pterygoid muscle*, Longus colli*, Longus capitis*, Anterior scalene muscle*, Middle scalene muscle*, Posterior scalene muscle*, Sternocleidomastoid muscle*, Rectus capitis anterior*, Rectus capitis lateralis*, Rectus capitis posterior major*, Rectus capitis posterior minor*, Obliquus capitis superior*, Obliquus capitis inferior*, Digastric muscle*, Stylohyoid muscle*, Mylohyoid muscle*, Geniohyoid muscle*, Sternohyoid muscle*, Omohyoid muscle*, Sternothyroid muscle*, Thyrohyoid muscle*
	Muscles of back (32)	Trapezius*, Latissimus dorsi*, Rhomboid major muscle*, Rhomboid minor muscle*, Levator scapulae*, Serratus posterior superior*, Iliocostalis lumborum*, Rest of iliocostalis*, Longissimus cervicis*, Longissimus capitis*, Rest of longissimus*, Rest of erector spinae*, Splenius capitis*, Transversospinalis*, Semispinalis cervicis*, Semispinalis capitis*
	Muscles of thorax & abdomen (24)	Pectoralis major*, Pectoralis minor*, Subclavius*, Intercostal muscle*, Diaphragm, Rectus abdominis*, External oblique abdominal muscle*, Internal oblique abdominal muscle*, Transversus abdominis*, Quadratus lumborum*, Levator ani, Coccygeus*
	Muscles of upper limb (82)	Deltoid muscle*, Supraspinatus*, Infraspinatus*, Teres minor*, Teres major*, Subscapularis*, Biceps brachii*, Coracobrachialis*, Brachialis*, Triceps brachii*, Anconeus*, Pronator teres*, Flexor carpi radialis*, Palmaris longus*, Flexor carpi ulnaris*, Flexor digitorum superficialis*, Flexor digitorum profundus*, Flexor pollicis longus*, Pronator quadratus*, Brachioradialis*, Extensor carpi radialis longus*, Extensor carpi radialis brevis*, Extensor digitorum*, Extensor digiti minimi*, Extensor carpi ulnaris*, Supinator*, Abductor pollicis longus*, Extensor pollicis brevis*, Extensor pollicis longus*, Extensor indicis*, Palmaris brevis*, Abductor pollicis brevis*, Flexor pollicis brevis*, Opponens pollicis*, Adductor pollicis*, Abductor digiti minimi*, Flexor digiti minimi brevis*, Opponens digiti minimi*, Lumbrical muscle*, Dorsal interosseus*, Palmar interosseus*
	Muscles of lower limb (98)	Iliopsoas*, Iliacus*, Psoas major*, Gluteus maximus*, Gluteus medius*, Gluteus minimus*, Tensor fasciae latae*, Piriformis*, Obturator internus*, Superior gemellus*, Inferior gemellus*, Quadratus femoris*, Sartorius*, Rectus femoris*, Vastus lateralis*, Vastus intermedius*, Vastus medialis*, Articularis genus*, Pectineus*, Adductor longus*, Adductor brevis*, Adductor magnus*, Gracilis*, Obturator externus*, Biceps femoris*, Semitendinosus*, Semimembranosus*, Tibialis anterior*, Extensor digitorum longus*, Extensor hallucis longus*, Fibularis longus*, Fibularis brevis*, Gastrocnemius*, Soleus*, Plantaris*, Popliteus*, Tibialis posterior*, Flexor digitorum longus*, Flexor hallucis longus, Extensor digitorum brevis*, Abductor hallucis*, Flexor hallucis brevis*, Adductor hallucis oblique head*, Adductor hallucis transverse head*, Abductor digiti minimi*, Flexor digiti minimi brevis*, Flexor digitorum brevis*, Quadratus plantae*, Plantar interosseus*
Skeletal (187)	Cranium (10)	Parietal bone, Frontal bone, Occipital bone, Temporal bone, Zygomatic bone, Lacrimal bone, Nasal bone, Maxilla, Mandible, Etc.
	Vertebral column (26)	First cervical vertebra, Second cervical vertebra, Third cervical vertebra, Fourth cervical vertebra, Fifth cervical vertebra, Sixth cervical vertebra, Seventh cervical vertebra, First thoracic vertebra, Second thoracic vertebra, Third thoracic vertebra, Fourth thoracic vertebra, Fifth thoracic vertebra, Sixth thoracic vertebra, Seventh thoracic vertebra, Eighth thoracic vertebra, Ninth thoracic vertebra, Tenth thoracic vertebra, Eleventh thoracic vertebra, Twelfth thoracic vertebra, First lumbar vertebra, Second lumbar vertebra, Third lumbar vertebra, Fourth lumbar vertebra, Fifth lumbar vertebra, Sacrum, Coccyx
	Thoracic skeleton (25)	First rib*, Second rib*, Third rib*, Fourth rib*, Fifth rib*, Sixth rib*, Seventh rib*, Eighth rib*, Ninth rib*, Tenth rib*, Eleventh rib*, Twelfth rib*, Sternum
	Bones of upper limb (64)	Scapula*, Clavicle*, Humerus*, Radius*, Ulna*, Scaphoid*, Lunate*, Triquetrum*, Pisiform*, Trapezium*, Trapezoid*, Capitate*, Hamate*, First metacarpal bone*, Second metacarpal bone*, Third metacarpal bone*, Fourth metacarpal bone*, Fifth metacarpal bone*, First proximal phalanx*, Second proximal phalanx*, Third proximal phalanx*, Fourth proximal phalanx*, Fifth proximal phalanx*, Second middle phalanx*, Third middle phalanx*, Fourth middle phalanx*, Fifth middle phalanx*, First distal phalanx*, Second distal phalanx*, Third distal phalanx*, Fourth distal phalanx*, Fifth distal phalanx*
	Bones of lower limb (62)	Hip bone*, Femur*, Patella*, Tibia*, Fibula*, Talus*, Calcaneus*, Navicular*, Medial cuneiform*, Intermediate cuneiform*, Lateral cuneiform*, Cuboid*, First metatarsal*, Second metatarsal*, Third metatarsal*, Fourth metatarsal*, Fifth metatarsal*, First proximal phalanx*, Second proximal phalanx*, Third proximal phalanx*, Fourth proximal phalanx*, Fifth proximal phalanx*, Second middle phalanx*, Third middle phalanx*, Fourth middle phalanx*, Fifth middle phalanx*, First distal phalanx*, Second distal phalanx*, Third distal phalanx*, Fourth distal phalanx*, Fifth distal phalanx*
Articular (23)	Vertebral joints (23)	Intervertebral disc (C II-C III), Intervertebral disc (C III-C IV), Intervertebral disc (C IV-C V), Intervertebral disc (C V-C VI), Intervertebral disc (C VI-C VII), Intervertebral disc (C VII-T I), Intervertebral disc (T I-T II), Intervertebral disc (T II-T III), Intervertebral disc (T III-T IV), Intervertebral disc (T IV-T V), Intervertebral disc (T V-T VI), Intervertebral disc (T VI-T VII), Intervertebral disc (T VII-T VIII), Intervertebral disc (T VIII-T IX), Intervertebral disc (T IX-T X), Intervertebral disc (T X-T XI), Intervertebral disc (T XI-T XII), Intervertebral disc (T XII-L I), Intervertebral disc (L I-L II), Intervertebral disc (L II-L III), Intervertebral disc (L III-L IV), Intervertebral disc (L IV-L V), Intervertebral disc (L V-Sacrum)

(continued to the next page)

cluding numerous surface models of a male cadaver. Another aim was to inform other researchers of the arranged methods to establish the PDF file of surface models.

MATERIALS AND METHODS

While users are able to open the PDF file simply on Adobe Reader, producers of the PDF file had to employ dissimilar software packages, depending on the procedures (Table 2).

Producing 3D surface models

We have been generating stereoscopic surface models from outlined images as part of the Visible Korean project for over 5 yr (Table 1). During this time, the surface reconstruction technique utilizing popular software has been continuously advancing (2, 4-10). In this article, we introduce the newest and most convenient approach, which uses Mimics version 10.01 (Materialise, Leuven, Belgium).

The outlines were filled with specific colors for the individual

 http://dx.doi.org/10.3346/jkms.2012.27.8.849

Table 1. *(continued from the previous page)* Six-hundreds forty-two surface models, categorized according to the systems and subsequent groups

Systems	Groups	Structures
Alimentary (49)	Teeth (28)	Medial maxillary incisor*, Lateral maxillary incisor*, Maxillary canine*, First maxillary premolar*, Second maxillary premolar*, First maxillary molar*, Second maxillary molar*, Medial mandibular incisor*, Lateral mandibular incisor*, Mandibular canine*, First mandibular premolar*, Second mandibular premolar*, First mandibular molar*, Second mandibular molar*
	Salivary glands & tongue (7)	Parotid gland*, Sublingual gland*, Submandibular gland*, Tongue
	Digestive tract (5)	Esophagus, Stomach, Duodenum, Jejunum & ileum, Large intestine
	Digestive glands (9)	Liver†, Common hepatic duct, Right hepatic duct, Left hepatic duct, Gallbladder, Cystic duct, Common bile duct, Pancreas, Pancreatic duct
Respiratory (14)	Nose (4)	Maxillary sinus*, Sphenoidal sinus*
	Trachea (1)	Trachea
	Lung & bronchi (9)	Right lung†, Left lung†, Right main bronchus, Right superior lobar bronchus, Right middle lobar bronchus, Right inferior lobar bronchus, Left main bronchus, Left superior lobar bronchus, Left inferior lobar bronchus
Urinary (6)		Kidney*, Ureter*, Urinary bladder (mural)†, Urinary bladder (luminal)
Genital (17)	Male internal genitalia (10)	Testis*, Epididymis*, Ductus deferens*, Seminal vesicle*, Ejaculatory duct, Prostate
	Male external genitalia (7)	Corpus cavernosum*, Corpus spongiosum, Superficial transverse perineal muscle*, Ischiocavernosus*
Endocrine (3)		Adenohypophysis, Neurohypophysis, Thyroid gland
Cardiovascular (34)	Heart (5)	Heart†, Right ventricle, Right atrium, Left ventricle, Left atrium
	Pulmonary arteries (3)	Pulmonary trunk, Right pulmonary artery, Left pulmonary artery
	Arteries of thorax & abdomen (8)	Ascending aorta, Arch of aorta, Brachiocephalic trunk, Descending aorta, Subclavian artery*, Common iliac artery*
	Arteries of head & neck (2)	Common carotid artery*
	Arteries of upper limb (6)	Axillary artery*, Brachial artery*, Radial artery*
	Arteries of lower limb (4)	External iliac artery*, Femoral artery*
	Veins (6)	Inferior vena cava, Common iliac vein, External iliac vein*, Femoral vein*
Lymphoid (1)		Spleen
Nervous (11)	Central nerves (5)	Spinal cord, Putamen*, Globus pallidus*
	Peripheral nerves (6)	Optic nerve*, Brachial plexus*, Sciatic nerve*
Sensory (4)	Eyes (2)	Eyeball*
	Ears (2)	External acoustic meatus*

Number of structures. *Both bilateral structures are surface reconstructed; †Surface is made semitransparent.

Table 2. Procedures for making the surface models and their PDF file, accompanied by necessary computer software

Procedures	Software (Resultant file formats)
1) Producing 3D surface models	Mimics (STL)
2) Embedding 2D surface models	Maya (STL)
3) Organizing surface models	Deep Exploration (VRML)
4) Putting surface models in PDF file	Acrobat (PDF)
5) Putting multimedia data in PDF file	Acrobat (PDF)
6) Assembling surface models	Acrobat (PDF)

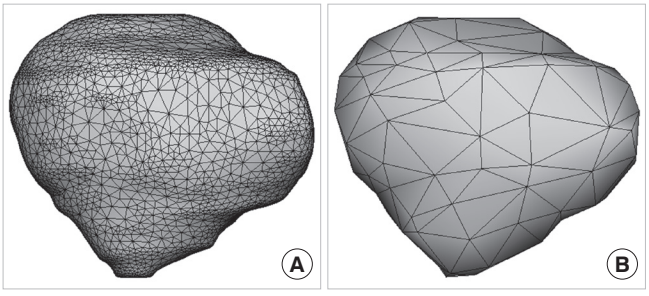

Fig. 1. The surface model of the patella with its mesh. (**A**) Full data. (**B**) Reduced data.

structures. The Mimics software recognized and clustered the serial outlines of each structure with the brightness of the colors. After stacking the outlines, surface reconstruction of all structures was simultaneously achieved (11-15). A problem was that the similar brightness of colors of neighboring structures interfered with the software recognition. To overcome this barrier, a set of outlines needed to be separated and reconstructed. If adjacent up-and-down outlines of a structure were not overlapped, automated surface reconstruction would not be carried out. In the case, contours of the structure were isolated and interpolated to make them overlap before the reconstruction (9).

The coincidentally constructed surface models were divided into a number of models of independent structures and saved as Mimics (MCS) files. They retained the structures' locational information. In each surface model, the accumulated outlines were removed and triangular surfaces were appropriately reduced in number. Inadequate surface models, resulting from incorrect outlining, were revised by anatomists (16).

To further reduce file size, the number of triangular surfaces was decreased as much as possible without compromising the original shape of the models. For very complicated structures (e.g., temporal bone), the surface was hardly reduced. The surface models prior to and after this simplification were designated as full data and reduced data, respectively (Fig. 1). File format of the composites of the reduced data was converted from MCS to stereolithography (STL), which is readable on Maya software.

Embedding 2D surface models

Using Maya software, we opened the 3D surface models (reduced data), into which serial 2D surface models including the sectioned images were inserted. For this job, 32 sectioned images through the entire body were chosen and basic structures were labeled on the images in advance. We elaborated 2D surface models that were the planes with no thickness and wrapped the prepared sectioned images in the models (Fig. 2). All matching 3D and 2D surface models were saved as STL files to be sent to the subsequent software.

Organizing surface models

Manipulation of the surface models would be facilitated if they were well-organized with an anatomic background. To this aim, Deep Exploration Standard (Right Hemisphere, San Ramon, CA, USA) was used to categorize the surface models into 13 systems. In each system, the models were grouped and arranged in official anatomical terms (Table 1) (17).

In this research, the about three-fourths of surface models originated from 286 muscles and 187 bones. For bones, following groups were appointed for subclassification: Cranium, Vertebral column, Thoracic skeleton, Bones of upper limb (Right), Bones of upper limb (Left), Bones of lower limb (Right), and Bones of lower limb (Left) (Table 1).

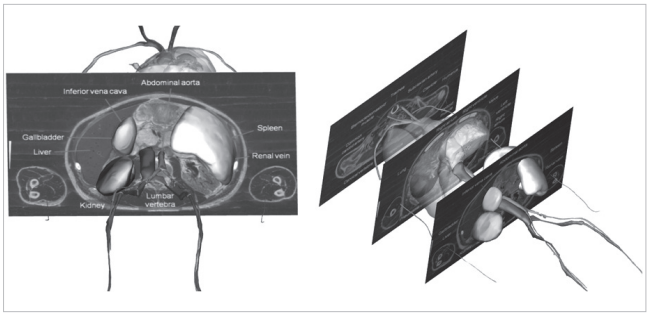

Fig. 2. Sectioned images with labels, embedded on the surface models.

The 2D surface models comprising the sectioned images were regarded as another system during this task. The 3D surface models were appropriately painted individually or by systems to distinguish the collective structures. The colors of skin, liver, lung, urinary bladder, and heart were made semitransparent to show their interiors (Fig. 3, Table 1). After finishing the coordination, all models were gathered in a single virtual reality modeling language (VRML) file.

Putting surface models in PDF file

This procedure was conducted on 3D Reviewer, the accompanying software of Acrobat 9.0 Pro Extended (Adobe Systems). The VRML file of adjusted surface models was inputted to a PDF file. As a result, the organization was displayed in the left top (model tree window) and surface models were exhibited in the right. During the input, spaces in the surface model name were automatically altered into underbars (e.g., Integumentary_system). Parentheses, unavoidably broken in this process, were recommended not to use (Fig. 3).

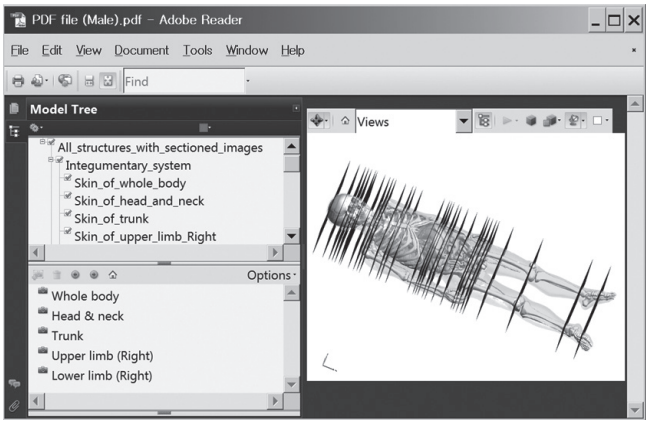

Fig. 3. Feature of PDF file, composed of the model tree window (left top), bookmark window (left bottom), and surface models (right). The surface models are colored with the skin made semitransparent.

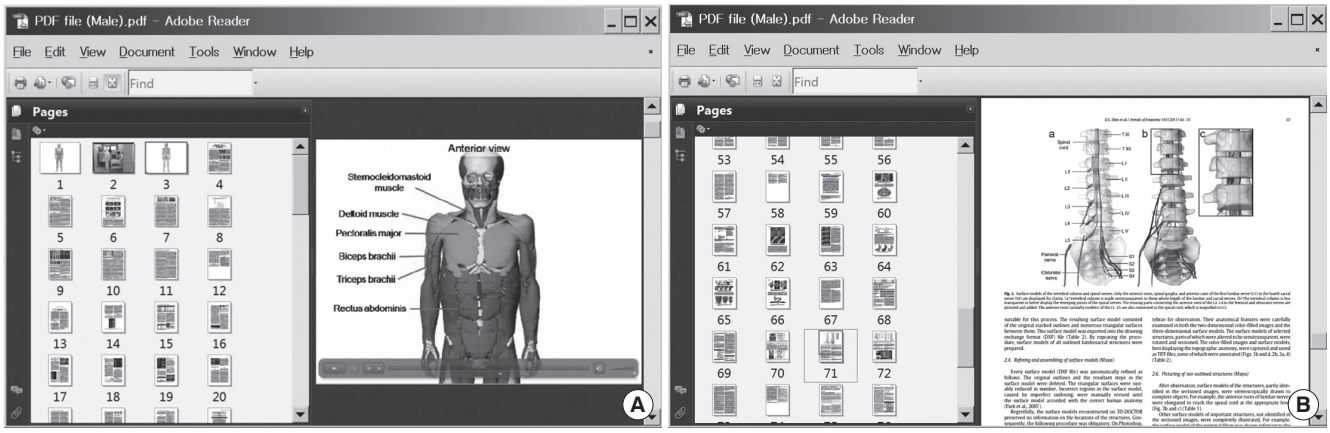

Fig. 4. Movie and paper introducing the surface models. (**A**) In the PDF files, the first and second movie is located on page 2 and 3, respectively. (**B**) The related articles are situated on the remnant pages.

http://dx.doi.org/10.3346/jkms.2012.27.8.849

Putting multimedia data in PDF file

Acrobat was used to attach multimedia data to the same PDF file. In this development process, a sound-enabled movie showing the serial sectioning of the cadaver to produce the sectioned images was made and attached to the PDF file. As well, the movie successfully presented the serially sectioned images at 1 mm intervals. Some of the sections were labeled as for the 2D surface models. A second movie recorded the labeled surface models of bones and muscles, which were displayed alternatively and rotated. The last data included were published articles, composed of texts and figures, explaining the sectioned images and surface models of the Visible Korean. In the PDF files, page 1 was already occupied by all surface models, and comprised the main contents. Therefore, the first and second movie was placed on page 2 and 3, respectively. The articles were put into the remaining pages (Fig. 4).

Assembling surface models

Retaining the systematic categorization of the surface models, it was advantageous for topographic anatomy that the models are assembled according to regions. So, using Acrobat, we created five bookmarks in the PDF file: Whole body, Head & neck, Trunk, Upper limb (Right), and Lower limb (Right) (Fig. 3). Every bookmark was the collection of surface models of the structures belonging to multiple systems. For example, 'Head & neck' was the assembly of models from integumentary, muscular, skeletal, articular, alimentary, respiratory, endocrine, cardiovascular, nervous, and sensory systems.

RESULTS

Prior to the present study, outlining and surface reconstruction had taken a decade to achieve. But the next main procedures in this research to attain an appropriate PDF file required just one week excluding the trial and error period (Table 2).

The PDF file (name, PDF file (Male).pdf; size, 73 MB) is available for download from the homepage of the Visible Korean project (http://anatomy.co.kr). Download is free and does not require registration. Surface models in the PDF file cannot be opened on other PDF viewers than Adobe Reader (Windows version). In the initial feature, surface models should be activated by clicking them once. All models can be closed by clicking the root check box on the model tree window. Successively users can generate mixed displays of structures using the check boxes of the systems, groups, and individuals for their intentions (Fig. 3 & 5, Table 1).

Two-dimensional surface models of sectioned images with labels can be exhibited as if they are items of another system. As a result, sectioned images can be superimposed on the 3D surface models (Fig. 2 & 3).

By use of the established bookmark window, desired regions such as 'Upper limb (Right)' can be displayed. Unlike the model tree, bookmark does not permit multiple choices (e.g., combination of 'Upper limb (Right)' with 'Trunk'). The selected region is spontaneously zoomed-in on the monitor to a suitable size, and rotating axes are established for the enlarged models (Fig. 6).

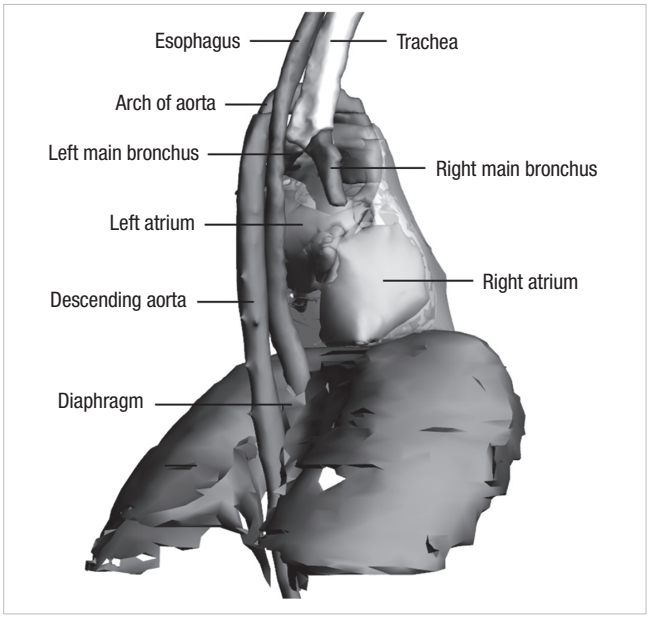

Fig. 5. Combination of the surface models showing the anatomical knowledge that esophagus is compressed by three structures: the arch of aorta, left main bronchus, and diaphragm.

When the user clicks a model, its anatomical name is highlighted in the model tree window. The second, third, and fourth clicks of the same model result in spotlighting of larger and larger groups involving the structure, until the entire systems are selected. Reverse highlighting is also possible; by clicking an interesting passage of text in the model tree window, the matching surface models in individual, group, or system are prompted for display (Fig. 6).

The surface models can be conveniently zoomed-in and zoomed-out by manipulating the mouse with the right button clicked or using the mouse wheel, and can be freely rotated with the left mouse button pushed. Moreover, models can be shifted with both the mouse left button and the keyboard Ctrl key depressed simultaneously.

The colors of surface models, already decided by developers, can be made semitransparent to better reveal aspects of the otherwise hidden surface models (Fig. 3). The intensity and color of illumination are capable of modification to enhance the stereoscopic effect. The Adobe Reader toolbar is available for diverse exploration of the surface models.

The supplementary multimedia data in the PDF file can be displayed by selection of the appropriate pages. The contents are likely to play a guide role of the whole surface models (Fig. 4).

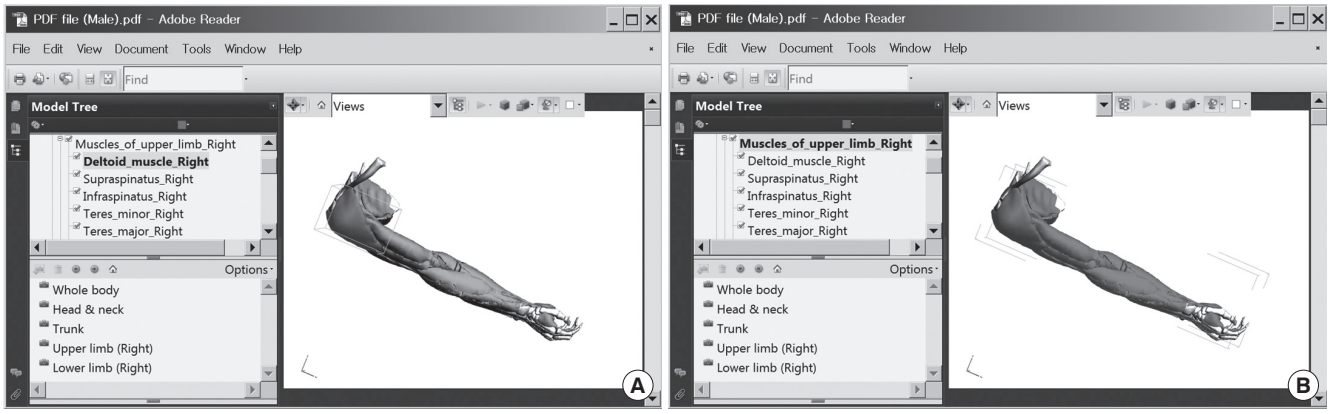

Fig. 6. Zoomed-in right upper limb region by selection of the bookmark 'Upper limb (Right).' (**A**) Highlighting of the surface model 'deltoid muscle' coincides with highlighting of the text 'deltoid muscle'. (**B**) Multiple clicks induce the spotlight of the muscular system including 'deltoid'.

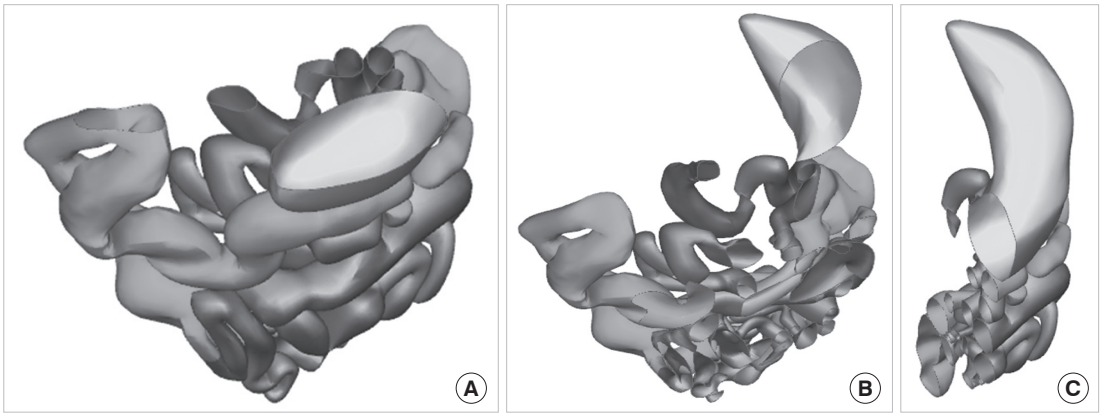

Fig. 7. Sectioning of the surface models of digestive tract. The horizontal (**A**), coronal (**B**), and sagittal (**C**) planes.

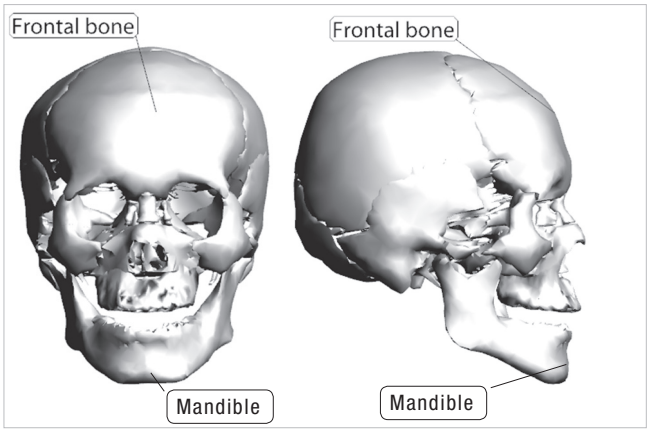

Fig. 8. Stereoscopic labeling on the surface models of frontal bone and mandible.

The functional variability of Acrobat enables the surface models in the PDF file to be visualized more powerfully. For example, the surface models can be cut to display their sectional planes. Horizontal sectioning yields the indigenous outlined images, which appear to be stuck to the surface models. Coronal, sagittal, and oblique sections are followed by new cutting edges of the surface models (Fig. 7).

Length and angle of the surface models can be measured. However, their surface area and volume are not amenable to analysis on Acrobat. Such analyses are possible using Rhinoceros, version 3.0 (McNeel North America, Seattle, WA, USA) or other software.

A surface model can be annotated stereoscopically. For labeling of each structure, one end of a line should be localized to be in contact with the surface; the other end needs to be decided for the label location. The term 'stereoscopically' denotes the linkage of the label and line with the surface model, even after its rotation. Labels can be written in English or other languages. In our experience, typing Korean letters necessitates use of the Korean version of Acrobat (Fig. 8).

The surface models can be extracted from the PDF file to accelerate other tasks. This is possible because the protection option was not invoked during the procedure to put surface models in PDF file on Acrobat. The extracted models are saved as STL, VRML, initial graphics exchange specification (IGES), Parasolid, or STEP, which can be accessed and modified by other 3D viewer software. Locational relationship of the adjacent struc-

http://dx.doi.org/10.3346/jkms.2012.27.8.849

tures is conserved after taking out the individual surface models of the PDF file.

DISCUSSION

A PDF file contains the 3D surface models of human anatomy and is opened on Adobe Reader (18, 19). The PDF file will hopefully be a learning tool of anatomy for various students, including children (Fig. 5). The unique feature of this study is that our surface models are sufficiently different from the ordinary ones to enable information-rich and educationally-valuable PDF file to be created.

Firstly, the surface models are objectively built based on scientific data. They are obtainable from outlining structures in serially sectioned images, stacking of these outlines, and using a polygon-based surface reconstruction method (16). The resultant elaborate models differ from currently available surface models that are generated by artists with knowledge of anatomy.

Secondly, the surface models are abundant in number. The 642 models made to date can be increased to 937, because 937 structures were delineated in the male cadaver (3). Moreover, real human color and high resolution of the sectioned images (pixel size, 0.2 mm; intervals, 0.2 mm), not obtainable from patients, allows extra outlining and further surface reconstruction of tiny constituents, which are a requisite for specific aims (5, 20). In the PDF file, a plethora of models are classified into systems and groups for the convenience of the user to search the individual structures and to display them jointly (Table 1). Besides, the bookmark option in the PDF file format can be used for further categorization of structures to represent body regions. The PDF format has the fascinating and beneficial function of being able to highlight both surface model and text. Both are emphasized, no matter which one is mouse-clicked (Fig. 6). This functionality is inevitably worthwhile, especially in cases of numerous models.

Thirdly, the surface models correspond to the state-of-the-art sectioned images. Combined demonstration is required because the sectioned images provide users with comprehensive information and, conversely, stereoscopic surface models help users grasp the native sectioned images (Fig. 2 & 3). In our primary attempt, the 2D sectioned images could not be placed over the 3D surface models in the PDF format. Therefore, we utilized 2D surface models containing the sectioned images. This innovative technique could be expanded to show the coronal and sagittal planes of sectioned images, as well as the outlined images from the same cadaver. Also, the sectioned images may be replaced with equivalent magnetic resonance imaging data and computed tomography images of the identical subject (1). The sectioned images on the 2D surface models might prove to be insufficient in terms of quantity and quality. To overcome this barrier, users can download from the browsing software of all the sectioned images and outlined images (intervals 1 mm) from the same homepage. The 2D system that supports surface models will satisfy various user demands (21). It is expected that the mixed demonstration of 3D surface models and 2D sectioned images will be developed and improved further by other investigators. For instance, the sectioned images are laid out successively at 1 mm intervals over the relevant surface models for more recognition. In case that this exceeds the extent of PDF function, computer reprogramming can be attempted to generate a different format file.

Fourthly, the surface models are accompanied by the associated multimedia data. Movies and scientific papers can be put into the different pages of the same PDF file (Fig. 4). The ability to have a single PDF file capable of supplying diverse types of data will undoubtedly facilitate its expedient use. This idea can be expanded to PDF files of journals. For example, relevant multimedia data supplied by the authors can be added to PDF reprint files, as a supplementary aid to readers (19).

Fifthly, the surface models are released as the raw data to promote various applications. Even though we did our best in the manufacture and organization of the surface models, the trial cannot satisfy all user needs. An ideal solution is to share the surface models with other developers. We do not hesitate to permit developers to extract the surface models from the PDF file, since our policy is the wide distribution of Visible Korean products (22). The surface models in PDF file are the reduced data for accelerating the operation speed on Adobe Reader. The full data of surface models are also to be distributed worldwide with no charge after agreement with the authors (Fig. 1). The same open-access policy is in place for the precursor data, the sectioned and outlined images. Those images in the browsing software are the reduced data; their full data also will be supplied (21). The full version of surface models and sectioned images could be a robust resource of virtual simulator for medical students or clinicians (7).

These five extraordinary characteristics of our own surface models are very compatible with the functions of PDF file and Adobe Reader. Indeed, that is why we investigated the potential availability of the PDF file. The PDF file may be progressively converted into many forms, including smart phone applications.

In summary, the main contribution of this study is to present a well-organized PDF file, where 3D and 2D surface models, as well as multimedia data, are browsed and utilized for medical learning. The technique to make the PDF file with 3D and 2D surface models, introduced in this paper, hopefully will aid other laboratories to produce PDF files carrying advantageous multimedia data.

REFERENCES

1. Park JS, Chung MS, Hwang SB, Lee YS, Har DH, Park HS. *Visible Korean Human. Improved serially sectioned images of the entire body. IEEE*

Trans Med Imaging 2005; 24: 352-60.
2. Park JS, Chung MS, Hwang SB, Lee YS, Har DH, Park HS. *Technical report on semiautomatic segmentation by using the Adobe Photoshop. J Digit Imaging 2005; 18: 333-43.*
3. Shin DS, Park JS, Park HS, Hwang SB, Chung MS. *Outlining of the detailed structures in sectioned images from Visible Korean. Surg Radiol Anat 2012; 34: 235-47.*
4. Shin DS, Chung MS, Lee JW, Park JS, Chung J, Lee SB, Lee SH. *Advanced surface reconstruction technique to build detailed surface models of liver and neighboring structures from the Visible Korean Human. J Korean Med Sci 2009; 24: 375-83.*
5. Shin DS, Park JS, Lee SB, Lee SH, Chung J, Chung MS. *Surface model of the gastrointestinal tract constructed from the Visible Korean. Clin Anat 2009; 22: 601-9.*
6. Jang HG, Chung MS, Shin DS, Park SK, Cheon KS, Park JS. *Segmentation and surface reconstruction of the detailed ear structures, identified in sectioned images. Anat Rec (Hoboken) 2011; 294: 559-64.*
7. Shin DS, Chung MS, Park JS, Park HS, Lee SB, Lee SH, Choi HN, Riemer M, Handels H, Lee JE, et al. *Three-dimensional surface models of detailed lumbosacral structures reconstructed from the Visible Korean. Ann Anat 2011; 193: 64-70.*
8. Shin DS, Park JS, Shin BS, Chung MS. *Surface models of the male urogenital organs built from the Visible Korean using popular software. Anat Cell Biol 2011; 44: 151-9.*
9. Shin DS, Chung MS, Park JS. *Systematized methods of surface reconstruction from the serial sectioned images of a cadaver head. J Craniofac Surg 2012; 23: 190-4.*
10. Shin DS, Park JS, Chung MS. *Three types of the serial segmented images suitable for surface reconstruction. Anat Cell Biol 2012; 45: 128-35.*
11. Lee YS, Seon JK, Shin VI, Kim GH, Jeon M. *Anatomical evaluation of CT-MRI combined femoral model. Biomed Eng Online 2008; 7: 6.*
12. Benkhadra M, Savoldelli G, Fournier R, Gamulin Z, François C, Trouilloud P, Feigl G, Fasel JH. *A new anatomical technique to investigate nerves by imagery. Surg Radiol Anat 2009; 31: 221-4.*
13. Yavuz MS, Buyukkurt MC, Tozoglu S, Dagsuyu IM, Kantarci M. *Evaluation of volumetry and density of mandibular symphysis bone grafts by three-dimensional computed tomography. Dent Traumatol 2009; 25: 475-9.*
14. Storck C, Juergens P, Fischer C, Haenni O, Ebner F, Wolfensberger M, Sorantin E, Friedrich G, Gugatschka M. *Three-dimensional imaging of the larynx for pre-operative planning of laryngeal framework surgery. Eur Arch Otorhinolaryngol 2010; 267: 557-63.*
15. Puchwein P, Schildhauer TA, Schöffmann S, Heidari N, Windisch G, Pichler W. *Three-dimensional morphometry of the proximal ulna. A comparison to currently used anatomically preshaped ulna plates. J Shoulder Elbow Surg 2012; 21: 1018-23.*
16. Park JS, Shin DS, Chung MS, Hwang SB, Chung J. *Technique of semiautomatic surface reconstruction of the Visible Korean Human data using commercial software. Clin Anat 2007; 20: 871-9.*
17. FCAT (Federative Committee on Anatomical Terminology). *Terminologia anatomica, international anatomical terminology. Stuttgart, New York: Thieme, 1998.*
18. Lanier L. *Advanced Maya texturing and lighting. Indianapolis: Wiley, 2008.*
19. Sahlin D. *How to do everything Adobe Acrobat 9. New York: McGraw-Hill, 2008.*
20. Park JS, Chung MS, Hwang SB, Shin BS, Park HS. *Visible Korean Human: Its techniques and applications. Clin Anat 2006; 19: 216-24.*
21. Shin DS, Chung MS, Park HS, Park JS, Hwang SB. *Browsing software of the Visible Korean data used for teaching sectional anatomy. Anat Sci Educ 2011; 4: 327-32.*
22. Park JS, Jung YW, Lee JW, Shin DS, Chung MS, Riemer M, Handels H. *Generating useful images for medical applications from the Visible Korean Human. Comput Methods Programs Biomed 2008; 92: 257-66.*

 http://dx.doi.org/10.3346/jkms.2012.27.8.849